Effect of In-Plane Density on the Structural and Elastic Properties of Graphite Intercalation Compounds

K. C. Woo
Moore School of Electrical Engineering and Laboratory for Research on the Structure of Matter, University of Pennsylvania, Philadelphia, Pennsylvania 19104

and

W. A. Kamitakahara
Ames Laboratory and Department of Physics, Iowa State University, Ames, Iowa 50011

and

D. P. DiVincenzo
Department of Physics and Laboratory for Research on the Structure of Matter, University of Pennsylvania, Philadelphia, Pennsylvania 19104

and

D. S. Robinson
Department of Physics and Materials Research Laboratory, University of Illinois at Urbana-Champaign, Urbana, Illinois 61801

and

H. Mertwoy, J. W. Milliken,[a] and J. E. Fischer
Moore School of Electrical Engineering and Laboratory for Research on the Structure of Matter, University of Pennsylvania, Philadelphia, Pennsylvania 19104

(Received 21 June 1982)

Dramatic differences in structure, elastic properties, and order-disorder temperatures are observed for stage-2 Li-graphite of different in-plane density, indicating the importance of long-range interactions in cohesive properties. LiC_{12} is three-dimensionally ordered up to ~ 500 K with $\sqrt{3} \times \sqrt{3}$ Li superlattice and AA graphite stacking, whereas LiC_{18} is disordered at 300 K and has AB stacking. LO and LA $(00l)$ phonon energies are 30% greater in the former, which can be understood in terms of electrostatic effects.

PACS numbers: 63.20.Dj, 61.12.Dw, 62.20.Dc

We report several dramatic differences in vibrational and structural properties between dense and dilute compounds of state-2 Li-graphite. Specifically, we have observed major differences in intercalate ordering, graphite stacking sequences, order-disorder temperatures, and $(00l)$ longitudinal phonon energies by means of neutron scattering measurements. The considerable recent interest in the ordering transitions of graphite intercalation compounds[1] (GIC) and the similarity of ordering and/or staging phenomena to those in related systems [e.g., rare gases absorbed on graphite[2] and intercalated transition-metal dichalcogenides[1] (ITMD)] impart a wider relevance to the results reported here.

GIC's generally progress from small to large intercalant density through staging. A stage-n compound consists of a sequence of n graphite layers and one intercalant layer repeated along the c axis. In contrast, most of the ITMD's are stage 1 at all accessible concentrations with continuously variable filling of the van der Waals gap. Several recent results[3,4] imply that stage-2 Li-graphite occurs with two different intercalant densities within the occupied van der Waals gaps, both of which are at least metastable at 300 K. It is the only known graphite system to do so. The unique possibility of exploring crystal structure, phase transitions, and lattice dynamics via neutron scattering in intercalation compounds of different in-plane stoichiometry is provided by our ability to synthesize large samples of Li-graphite. The ITMD's can only be prepared in the form of powder or small crystals and are thus not amenable to lattice dynamics studies by neutron scattering. The present work represents the first such study of an intercalation compound as a function of in-plane density.

Stage-2 Li-graphite is prepared in two distinct colors, pink and blue, by immersing Union Carbide highly oriented pyrolytic graphite (HOPG) or Goodrich pyrolytic graphite (PG) in molten Li/Na alloy. We used 99% enriched ^{7}Li. The blue samples[5] are grown in 3.5 mol% Li at 200–300 °C while pink is obtained with 5–6% Li at 400 °C. Other reaction conditions[4] as well as the vapor-phase technique[3] also appear to give two distinct phases. Experiments were carried out on both HOPG and PG samples using a triple-axis spectrometer at the Oak Ridge high-flux isotope reactor with fixed incident neutrons of 14.77 meV or fixed neutron final energy of 13.65 meV. The HOPG and PG samples had about 5° and 12° mosaic spread after intercalation, respectively. The samples were packaged in stainless-steel envelopes.[6] Results were identical for both types of starting materials; most of the inelastic data were obtained from the larger PG samples.

The Drude edges of the pink and blue materials are 2.6 and 1.45 eV, respectively, indicating that the pink samples have higher in-plane Li density.[7] DiCenzo, Basu, and Wertheim[8] conclude from x-ray photoemission core-level intensities that blue samples have a chemical formula $LiC_{18\pm1}$. In this work, we observe a $\sqrt{3}\times\sqrt{3}$ Li superlattice for pink samples, consistent with Guerard's original report on stage-2 Li-graphite of unspecified color[9] and with more recent data of Billaud *et al.*[4] on stage-2 Li-graphite described as blue. We find that the pink color degrades superficially towards blue even in clean argon atmosphere, so that Billaud's blue material can reasonably be considered to be the same as Guerard's stage-2 and our pink compound. The $\sqrt{3}\times\sqrt{3}$ Li superlattice implies an ideal chemical formula LiC_{12}. Using the intensity of Li(100), Li(200), and graphite(100) reflections,[10] we estimate that the pink samples used in this work are $LiC_{13.5\pm1.5}$. Weight-uptake measurements are unreliable because of variable amounts of alloy which occupy gross defects in the starting material.[5] The repeat distances of LiC_{12} and LiC_{18} were found to be 7.024 and 7.055 $\pm$ 0.005 Å, respectively, consistent with stronger interlayer Li-C Coulomb interaction in the denser phase. Similar effects are observed in overcharged acceptor compounds.[11] Intermediate compositions either do not exist or are much less stable. In samples with overall Li concentrations between LiC_{18} and LiC_{12}, two distinct phonon branches characteristic of the pure phases are detected, suggesting separation into blue and pink phases.

Figure 1 is a schematic representation of the elastic scattering results. For LiC_{12} at 295 K $(h\,00)$ scans reveal cylindrically averaged (100) and (200) reflections from the $\sqrt{3}\times\sqrt{3}$ Li superlattice, while the $(10l)$ and $(\sqrt{3}\,0l)$ scans confirm[9,12] the unusual $\alpha AA\alpha AA\cdots$ stacking. In contrast, no Li reflections are found in LiC_{18}, and the $(\sqrt{3}\,0l)$ scan shows a doubling of the unit cell along $\bar{c}$ indicating $AB/BA/AB\cdots$ stacking. This sequence is locally similar to graphite $(ABAB\cdots)$ but different globally from all other stage-2 alkali GIC's $(AB/BC/CA\cdots)$.[1] The same diffractogram is found for LiC_{18} quickly cooled to 10 K, implying either that the order-disorder transition (if any) occurs below 10 K or that the ordering process takes place very slowly below 300 K. In contrast, LiC_{12} disorders at $T_0 \sim 500$ K; the corresponding process in stage-1 LiC_6 ($\alpha A\alpha A$ stacking) occurs at[6,12] 715 K. Intensity estimates for various ordered LiC_{18} phases indicate that their reflections would have been observable in the $(h\,0l)$ scans had they existed. Details of the phase transitions will be presented elsewhere.

The Li-graphite system is unique in that one must invoke attractive interlayer Li-Li interactions, in addition to the repulsive elastic and/or electrostatic interlayer interactions,[13] in order to arrive at an eclipsed intercalant stacking se-

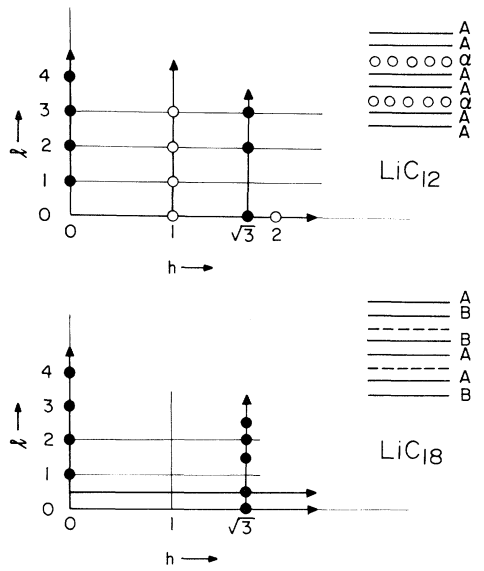

FIG. 1. Schematic reciprocal-space diagram for LiC_{12} at 295 K and LiC_{18} at 10 K, indicating the scans performed (heavy lines) and the reflections observed (filled circles: predominantly graphite reflections; open circles: Li reflections). Indexing is in units of the LiC_{12} cell. Implied structures are shown as insets.

quence in LiC_6. This attractive component must be fairly long range because it is still important in the stage-2 compound LiC_{12}. Since LiC_6 and LiC_{12} have the same in-plane structure and intercalant stacking, the ~200 K difference in T_0's is a rough measure of the difference between the net Li-Li interlayer interaction acting at distances of 3.7 and 7.0 Å. Even at the larger distance, this interaction is apparently strong enough to override the C-C interlayer interaction, forcing the unusual AA sequence as long as the Li's are locked to their C neighbor layers. In LiC_{18}, on the other hand, either the lower density or the absence of a commensurability term reduces the Li-C nearest-layer coupling such that the C-C nearest-layer interaction (which favors AB stacking) takes over, yielding the usual graphitic sequence. This weak Li-C coupling may be a factor contributing to the lower T_0 of LiC_{18}.

Figure 2 shows the measured $(00l)$ phonon dispersion for LiC_{12} and LiC_{18}, along with the fits of a one-dimensional nearest-neighbor force-constant model which we discuss later. The phonon energies are ~30% greater in the denser material. Since the two branches observed are primarily graphitelike,[14] we are directly probing the effect of intercalant density on the host elastic properties transverse to the layers. To the best of our knowledge, this is the first time that such an experiment has been possible. The low-frequency slopes yield sound velocities v_s and compressibilities k_{tot} as follows: 5.56×10^5 cm/sec and 2.69×10^{-12} cm^2/dyn for LiC_{12}; 4.07×10^5 cm/sec and 1.42×10^{-12} cm^2/dyn for LiC_{18}. These values, along with previous data[15] on MC_{24} (M = K, Rb, Cs), are consistent with a simple model for the elastic energy, in which the contribution of the two adjacent C layers k_c is graphitic and the C-I-C sandwich is represented by an electrostatic term k_i. The composition law gives $k_{tot} = (c_i k_i + c_c k_c)/(c_i + c_c)$, where c_i and c_c are the appropriate layer separations, 3.70 and 3.35 Å, respectively. We estimate the concentration dependence of k_i as follows. The electrostatic energy for the C-I-C sandwich has recently been shown to be[16] $E_{es} \propto A_0 \sigma^2 c_i$, where σ is charge/area and A_0 is area per I atom. The electrostatic and total energies for the sandwich are related by[17] $\partial E_{es}/\partial c_i = 3c_i\,\partial^2 E_{tot}/\partial c_i^2$. But the sandwich compressibility is defined as $k_i = (A_0/c_i)(\partial^2 E_{tot}/\partial c_i^2)^{-1}$. Combining these equations gives the particularly simple result $k_i \propto \sigma^{-2}$; i.e., k_i decreases with the inverse square of the concentration (assuming unity charge transfer). Interestingly, k_i is independent of sandwich thickness c_i. These results combined with the composition law predict a linear relationship between the experimentally measured quantities plotted in Fig. 3, with an intercept equal to the graphite value. The fact

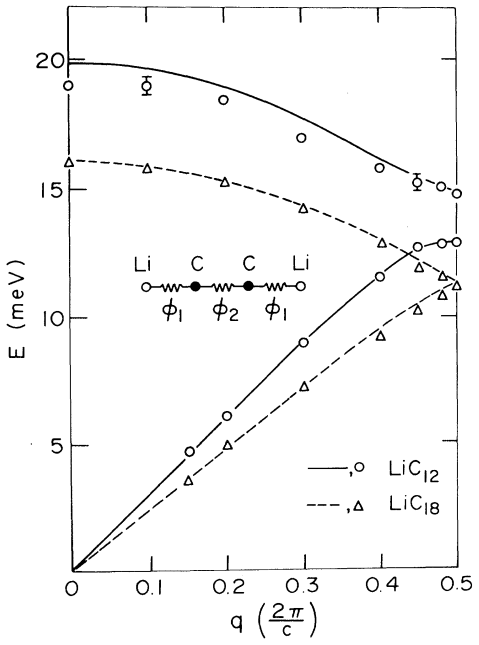

FIG. 2. Experimental $(00l)$ phonon dispersion for LiC_{12} (circles) and LiC_{18} (triangles). Solid and dashed curves are the corresponding fits of a nearest-neighbor force-constant model (Ref. 15), shown as an inset.

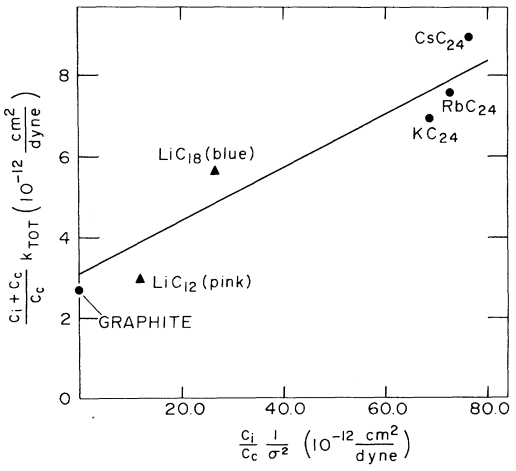

FIG. 3. Scaled compressibilities vs the scaled inverse square of intercalant concentration for stage-2 alkali GIC's. Solid line is the electrostatic model result described in the text and the symbols are from neutron data (present work plus Ref. 15).

that these predictions agree with all the available data[15] to within 10% indicates that the interlayer C-*I* interaction is indeed primarily electrostatic.

We attempted to analyze the data of Fig. 2 with a nearest-neighbor force-constant model, motivated by its successful application to the lower graphitelike acoustic and optic branches of stage-2 and -3 heavy alkali compounds.[18] The fit to LiC_{18} is good, yielding $\varphi_1 = 5750$ dyn/cm and $\varphi_2 = 3000$ dyn/cm for C-Li and C-C force constants, respectively. In contrast, the LiC_{12} fit is poor for the optic branch (Fig. 2). Further evidence of the failure of this model for LiC_{12} is that $\varphi_2 = 4070$ dyn/cm is unphysically large, whereas the four dilute disordered stage-2 GIC's (LiC_{18}, MC_{24}) give φ_2 values comparable to graphite (as would be expected from a nearest-neighbor model). Zabel and Magerl[15] subsequently found it necessary to use a mixed one-dimensional ion shell/Born–von Karman model to fit the upper alkalilike optic branches of MC_{24} and KC_{36}. While this latter model might also produce a better fit to the lower optic branch of LiC_{12}, it is significant that LiC_{12} is the only stage-($n \geq 2$) compound for which the nearest-neighbor force-constant model does not fit all the graphitelike branches reasonably well. This failure could result from the greater charge density ($\frac{1}{6}e$ per C in LiC_{12} vs $\frac{1}{9}e$ per C and $\frac{1}{12}e$ per C in LiC_{18} and MC_{24}, respectively, assuming M^+ in all cases) or from the long-range interactions implied by the structural data.

The C-Li force constant $\varphi_1 = 10\,040$ dyn/cm for LiC_{12}, twice that found for LiC_{18}. This difference could be partially due to the inadequacy of the nearest-neighbor model, although it is consistent with stronger interlayer interactions as deduced from the structural and T_0 arguments as well as with the greater in-plane density.

The dramatic differences observed in the elastic, structural, and order-disorder behavior of the two stage-2 compounds LiC_{12} and LiC_{18} result from a complex interplay of in-plane density, commensurability, and interlayer interactions beyond nearest neighbors. Similar differences in electronic properties probably exist. Compounds of Li-graphite with stage >2 have been reported[4]; it is not presently known if they too exist with different in-plane densities. Detailed studies of Li-graphite may help to explain why staging dominates in GIC's while variable in-plane density is the rule in ITMD's.

This work was supported by the Army Research Office under Contract No. DAAG29-80-K-0019 and by the Department of Energy under Contract No. W-7405-Eng-82; Oak Ridge National Laboratory is operated by Union Carbide under Department of Energy Contract No. W-7405-Eng-26. Sample preparation was supported by the National Science Foundation–Materials Research Laboratory Program under Contract No. DMR-7923647 and No. DMR-8020250. We are grateful to Dr. H. Zabel for helpful discussions and preprints of Refs. 15 and 18. We acknowledge the assistance of Dr. R. M. Nicklow and Dr. N. Wakabayashi and the generosity of Dr. A. W. Moore of Union Carbide in providing the HOPG.

---

[a]Current address: Naval Research Laboratory, Washington, D. C. 20375.

[1]For recent reviews, see Physica (Utrecht) 99B (1979), 105B+C (1981); S. A. Solin, Adv. Chem. Phys. 49, 455 (1982).

[2]*Ordering in Two Dimensions*, edited by S. K. Sinha (North-Holland, Amsterdam, 1980).

[3]P. Pfluger, V. Geiser, S. Stolz, and H. J. Guntherodt, Synth. Met. 3, 27 (1981).

[4]D. Billaud, E. McRae, J. F. Mareche, and A. Herold, Synth. Met. 3, 21 (1981).

[5]S. Basu, C. Zeller, P. Flanders, C. D. Fuerst, W. D. Johnson, and J. E. Fischer, Mater. Sci. Eng. 38, 275 (1979).

[6]D. S. Robinson and M. B. Salamon, Phys. Rev. Lett. 48, 156 (1982).

[7]P. Pfluger, K. P. Ackermann, R. Lapka, E. Schupfer, P. Jeker, H. J. Guntherodt, E. Cartier, and F. Heinrich, Synth. Met. 2, 285 (1980).

[8]S. B. DiCenzo, S. Basu, and G. K. Wertheim, Synth. Met. 3, 139 (1981).

[9]D. Guerard and A. Herold, Carbon 13, 337 (1975).

[10]G. E. Bacon, *Neutron Scattering* (Oxford Univ. Press, London, 1955), p. 89. We assumed the Debye-Waller factor to be $B \sin^2\theta$, where B is inversely proportional to mass and θ is the Bragg angle.

[11]A. Metrot and J. E. Fischer, Synth. Met. 3, 201 (1981).

[12]A. Wiedenmann and J. Rossat-Mignod, unpublished.

[13]S. A. Safran, Synth. Met. 2, 1 (1980).

[14]Preliminary data indicate a dispersionless Li branch at 28 ± 1 meV for both LiC_{12} and LiC_{18}.

[15]H. Zabel and A. Magerl, Phys. Rev. B 25, 2463 (1982).

[16]D. P. DiVincenzo and E. J. Mele, Phys. Rev. B 25, 7822 (1982).

[17]Obtained by differentiating the virial theorem, neglecting exchange and correlation.

[18]A. Magerl and H. Zabel, Phys. Rev. Lett. 46, 444 (1981).